Ordered Stacking of F-Actin Layers and Mixed Lipid Bilayers: A Columnar Liquid Crystal

A. Caillé,[1] F. Artzner,[2] and F. Amblard[3]

[1]*Département de Physique, Université de Montréal, Montréal, Canada H3C3J7*
[2]*Institut Physique de Rennes, UMR 6251 CNRS, Université de Rennes 1, 35042 Rennes Cedex, France*
[3]*Laboratoire de Physico-chimie, UMR 168 CNRS, Institut Curie, 75248 Paris Cedex 04, France*

(Received 30 July 2012; published 22 January 2013)

In this Letter, we show how the grooved helical structure of actin microfilaments (F-actin) interacting with mixed fluid lipid bilayers leads to handedness-independent 1D lipid bilayer undulations coupled to longitudinal in-plane ordering of the microfilaments. This longitudinal ordering is forced by the emerging in-plane compression and curvature energy terms of the straight 1D bilayer undulation wave fronts. Thereby, adjacent helices are set into registry along their long axis in their monolayer and π shifted between adjacent monolayers. An ordered composite multilamellar structure emerges by alternate stacking of these lipid bilayers and monolayers of F-actin. This two-dimensionally ordered system has the symmetries of a centered rectangular columnar liquid crystal, the straight 1D wave fronts playing the role of the classical molecular columns.

DOI: 10.1103/PhysRevLett.110.048102 PACS numbers: 87.15.bk, 61.30.−v, 64.75.Yz, 68.65.Ac

How soft composite structures emerge by self-assembling lipid bilayers and rigid biopolymers is of interest to understand various phenomena such as DNA packaging for gene transfer and therapy [1], the crystallization in such self-assembled composite templates of inorganic nanoparticles with unexpected physical properties in 1D and 2D assemblies [2,3], and the interactions between cell membranes and the cytoskeleton (F-actin) that drive various cellular organizations [4]. The above phenomena all have a common dimension. They combine molecular structures of distinct internal symmetries: the planar two-dimensional isotropic fluid lipid bilayers and the one-dimensional helical structure of most biopolymers. In the above context, the mixed (neutral and cationic) lipid bilayers and lambda DNA complex, one of the most studied self-assembled soft matter lamellar complexes, sustains structural phases [5–12] with intermolecular ordering of DNA which develops transversally to the DNA strands, the DNA helical symmetry having no consequences and longitudinal translations being free.

More recently, the structural properties of the lamellar complex of F-actin and mixed lipid bilayers have been measured in two studies with different ordered phases being reported for each study. This discrepancy might result from the selection of different pathways for their self-assembly. The first experimental data [13] were interpreted as a lamellar stack of ''three-layer'' composite superlayers: a lipid bilayer sandwiched between two monolayers of F-actin. Synchrotron x-ray diffraction data were then interpreted as those of a one-dimensional lamellar superlattice of the suggested ''three-layer'' superlayers. More recently, a second self-assembled structure [3] was published for this complex in the context of the crystallization of inorganic quantum dots within its lamellar phase. The structure, without quantum dots, was studied using detailed SAXS diffraction experiments from highly oriented fibers. The Bragg peaks were interpreted with high precision as resulting from 2D lattice ordering with short range ordering in the third perpendicular direction. The hk plane of the 2D lattice [Fig. 1(a)] has the centered rectangular systematic extinction rule, $h + k = 2n + 1$, with cell dimensions $2a$ and b being, respectively, equal to 25 and 38 nm. b is very close to half of the helical pitch of F-actin and $2a$ is approximately twice the thickness of a ''two-layer'' superlayer made of one lipid bilayer (4 nm) and one monolayer of roughly parallel F-actins (8.8 nm) where, inside each monolayer, the hills and valleys of the F-actin are set in phase in the F-actin axis direction [Figs. 1(c) and 2]. High-resolution SAXS profiles show an additional diffused scattering peak perpendicular to the hk plane, attributed to short range ordering perpendicular to the F-actin inside the monolayers. A simple structural model then emerges where the unit cell perpendicular to the lipid bilayer is composed of two ''two-layer'' superlayers, the helical intramolecular structure [Fig. 1(a)] of the in-phase F-actins being longitudinally π shifted between adjacent superlayers. Indication of the longitudinal locking inside each F-actin monolayer is obtained from freeze fracture electron microscopy in the lamellar phase. Indeed, a two-dimensional rectangular deformation pattern of the lipid monolayer is observed [3] with perpendicular carved grooves with respective spatial periods of 35 and 15 nm, the 35 nm period revealing the in-phase longitudinal locking of the F-actin and the 15 nm period the average perpendicular distance between F-actin in their monolayer. The above 2D long range positional ordering in a three-dimensional material absolutely calls nevertheless for a yet unrevealed mechanism to lock in-phase adjacent F-actins inside each ''two-layer'' superlayer. This is the central contribution of the present Letter.

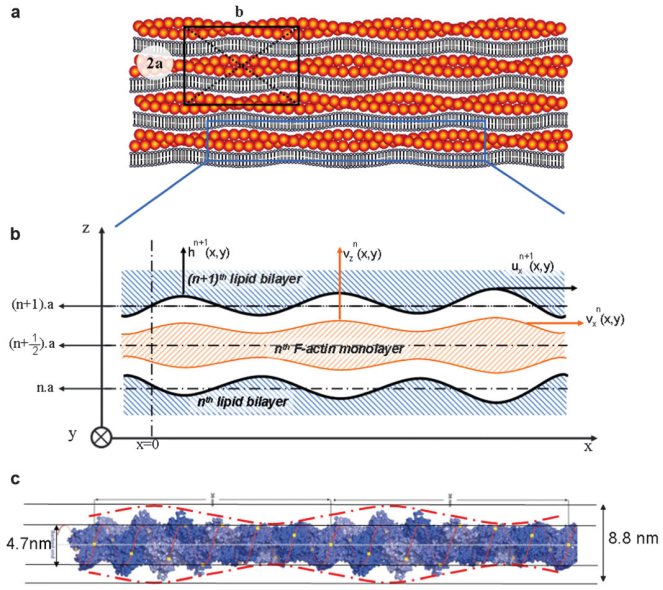

FIG. 1 (color). (a) A stack of F-actin monolayers and undulated lipid bilayers with the 2D centered rectangular conventional unit cell. (b) Expanded view showing the $(n+1)$th and nth lipid bilayers intercalated with an in-phase nth F-actin monolayer represented by its sinusoidal limiting boundaries. $u_x{}^{n+1}(x, y)$ and $h^{n+1}(x, y)$ are the elastic fluctuations in the x and z direction of the $(n+1)$th lipid bilayer. $v_x{}^n(x, y)$ and $v_z{}^n(x, y)$ are similar fluctuations for the undulated nth F-actin monolayer, and (c) cross section of the high-resolution molecular structure inferred from electron microscopy [18]. A simplified representation kindly provided by R. Dominguez [19] shows the typical short pitch left-handed helix, together with the best fit of the projected contour by a harmonic undulation with diameters ranging from 4.7 to 8.8 nm.

The simplifying assumptions of our model are briefly reviewed. First, we disregard deformations having a modulation of membrane thickness and only consider undulations at constant thickness because over the same length scale the former costs an order of magnitude more energy than the latter. The determination of the molecular structure of F-actins has been a true challenge over the last three decades [14–16]. Recent x-ray fiber diffraction and electron cryomicroscopy studies have confirmed a now widely accepted structure [17–19] at the nearly atomic resolution needed for our work. These studies all agree that the molecular structure of F-actin is that of a single left-handed helix with approximately 13 actin molecules repeating every six turns for an axial distance of the order of 36 nm [Fig. 1(c)]. From a different perspective, the molecular structure of F-actin appears to be made up of two right-handed necklaces of beads, intertwined as a 72 nm-pitch helix. In an axial cross section, the molecular structure extends in width from approximately 8.8 to 4.7 nm [18]. F-actin can be schematically viewed by analogy with a mechanical drill as follows: an 8.8 nm diameter cylinder carved with two opposed right-handed grooves with a 2 nm depth and a 72 nm pitch, leading to an effective 36 nm period. As a result, the projected diameter of F-actin, in a cross-section plane, undulated between 4.7 and 8.8 nm within the 36 nm period. In agreement with the highest resolution (0.68 nm) data published to date [18,19], this undulation is modeled here by sinusoidal boundaries [Fig. 1(c)]. In this Letter, we disregard the biochemical polarity of F-actin, both ends being considered as geometrically identical. The rigid F-actin microfilaments are also considered to be parallel inside each monolayer.

A mixture of neutral and cationic lipids is necessary to set into action the entropic forces driving a self-assembly mechanism. The mixed nature of the lipids could affect the detailed form of the interaction potential V identified in (5), in particular, through a lateral phase separation of neutral and cationic lipids [20] which would generate a position-dependent Deryagin potential V. This effect is not treated in this Letter. Two configurations of parallel microfilaments within a monolayer are considered: (a) equidistant microfilaments with a transversal separation of 15 nm but no longitudinal ordering and (b), in-phase microfilaments with their 36 nm period locked in phase (Fig. 2) inside the monolayer with only short range in the transversal distance between microfilaments (average distance being $c \approx 15$ nm). The landscapes of both configurations can be well matched geometrically by a single wavelength undulation of the lipid bilayer with straight 1D stationary wave fronts, either parallel (a) or perpendicular (b) to the F-actin axis. Note that the fluctuations in the transversal distances between F-actin microfilaments in case (b) do not affect the straight nature of the wave fronts. The out-of-plane bending energy of the lipid bilayer is inversely proportional to (wavelength)^4, the cost in bending energy is roughly 30 times smaller for longitudinal order (b) than for transversal order (a). Assuming that the transition from a disordered F-actin monolayer (with longitudinal and transversal disorders) to an ordered monolayer is first initiated by the growth of a single wave number undulation, configuration (b) wins over (a) to determine the

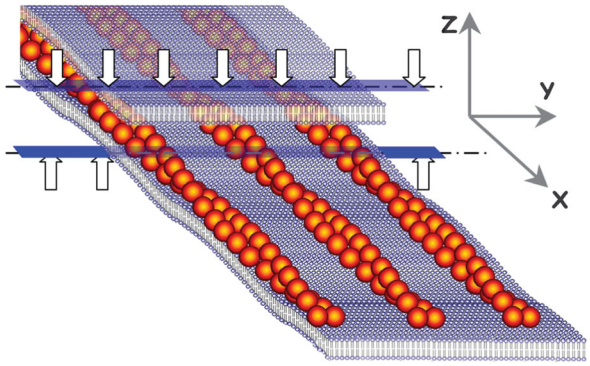

FIG. 2 (color). Three F-actin microfilaments laying on an undulated lipid bilayer with their hills and valleys in phase along the x direction, the arrows pointing upward and downward indicating the pinching undulation of the two neighboring lipid bilayers. The blue stripes (with the inscribed dashed line) in the y direction represent the straight 1D wave front.

most ordered phase. Without further developments, we retain configuration (b) with longitudinally ordered in-phase (as in Fig. 2) parallel F-actin microfilaments in each monolayer as the most ordered configuration.

The undulated lipid bilayers and the longitudinally in-phase ordered F-actin monolayers [Figs. 1(b) and 2], both of wave number q^o_x, are taken to form continuous surfaces in the x-y plane. The fluctuating z coordinate of the $(n+1)$th undulated lipid bilayer is [Fig. 1(b)]:

$$H^{n+1}(x,y) = h^{n+1}(x,y) + (n+1)a + \Psi^{n+1}\exp\{iq^0_x[x - u_x{}^{n+1}(x,y)]\} + \text{c.c.}, \quad (1)$$

$u_x{}^{n+1}(x,y)$ and $h^{n+1}(x,y)$ being, respectively, elastic fluctuations in the x and z direction. The x-z axial cross section of the in-phase ordered nth F-actin monolayer is bordered by $H_a{}^{n\pm}(x,y)$ given by [Fig. 1(b)]:

$$H_a{}^{n\pm}(x,y) = \upsilon_z{}^n(x,y) + (n+1/2)a \pm d/2 \pm \Phi^n\exp\{iq^o_x[x - \upsilon_x{}^n(x,y)]\} + \text{c.c.}, \quad (2)$$

d is the mean diameter of the F-actin ($d \approx 6.75$ nm) and elastic fluctuations $\upsilon_x{}^n(x,y)$ and $\upsilon_z{}^n(x,y)$ are introduced. Ψ^n and Φ^n are, respectively, the lipid bilayer undulation amplitude and the amplitude of undulation of the microfilament radius. The amplitudes Ψ^{n+1} and Φ^n, with $\Psi^{n+1} = \Psi/2\exp\{-i\pi(n+1/2)\}$, are chosen to ensure a centered rectangular 2D lattice in the z-x plane. With $h_0 = a/2 - d/2$, the static coordinates of the $n+1$th lipid bilayer, $H_s{}^{n+1}(x,y)$, and of the nth F-actin monolayer, $H_{as}{}^{n+}(x,y)$, are, respectively,

$$H_s{}^{n+1}(x,y) - (n+1/2)a - d/2 = h_0 + h_s{}^{n+1}(x,y), \quad (3)$$

$$H_{as}{}^{n+}(x,y) - (n+1/2)a - d/2 = h_{as}{}^{n+}(x,y). \quad (4)$$

The energy functional of a "two-layer" superlayer of a tensionless fluid lipid bilayer of constant thickness (taken to be zero) and bending rigidity K_b (typically $2.4k_BT$) interacting strongly with the ordered F-actin monolayer through a potential $V(H_s, H_{sa})$ is

$$F[h_s] = \iint dxdy\{1/2\mathrm{K}_b[\nabla^2(h_s)]^2 + V_0 + 1/2k(h_s - h_{sa})^2\}. \quad (5)$$

V results from the attractive electrostatic potential and short range repulsive hydration forces typical of a strongly adhering mixed lipid membrane on a protein surface separated by a salt-free aqueous layer with full entropic release of the counterions. V is expanded harmonically around its local minimum V_0 with the restoring force constant k. With $\mathbf{q}_2 = q_x\mathbf{i} + q_y\mathbf{j}$, the energy functional (5) is minimized [21] for

$$h_s{}^e(\mathbf{q_2}) = h_{sa}(\mathbf{q_2})/(1 + \xi^4|q_2|^4). \quad (6)$$

The correlation length ξ ($\xi^4 = \mathrm{K}_b/k$) characterizes the crossover between the bended to flat lipid bilayer regimes. For static straight 1D wave fronts of undulation defined by $h_{sa}(x)$ equal to $\Phi\sin(q^o_x x)$, we get $h_s{}^e(x)$ equal to $fh_{sa}(x)$, with f equals to $[1/(1 + \xi^4 q^o{}_x{}^4)]$. f measures the extend by which the lipid bilayer follows the undulation imposed by the in-phase ordered F-actin monolayer. Values of ξ smaller or equal to b ($b = 2\pi/q^0{}_x$) favor the appearance of static straight 1D wave fronts in the lipid bilayer. A good estimate of ξ is accessible in the strongly adhering limit where the spacing between lipid head groups and F-actin monolayer is a fraction of a nanometer. k is then estimated to be $0.2(k_BT)/\mathrm{nm}^4$ for V dominated by an attractive electrostatic contribution and a short range repulsion due the entropic effect of water molecules inserted between the lipid heads [22]. Under these conditions, $\xi = 1.8$ nm ($b = 36$ nm) and f equals 0.99. This confirms that for the actin case, the fluid lipid bilayer adopts a static strongly undulated structure in the ordered phase. Similar estimate for a DNA-lipid bilayer complex to set into longitudinal in-phase registry with a period of the order of 3.4 nm points to a value $f \approx 10^{-3}$, clearly showing that the above mechanism is not favored in this last case, leading to transversal ordering of the DNA strands [6].

It is easily shown that the elastic fluctuation free energy, measured relative to the static configuration of wave number q^0_x (6), of an undulated lipid bilayer interacting with an F-actin monolayer has the following new nonzero emerging terms to second order:

$$F_{\text{elas}} = \iint dxdy\{1/2\mathrm{K}_b[\nabla^2 h(x,y)]^2 + 1/4f^2\mathrm{K}_b(\Phi q_x{}^o)^2 \times [\partial^2 u_x(x,y)/\partial y^2]^2 + \frac{3}{2}f^2\mathrm{K}_b(q_x{}^o)^2(\Phi q_x{}^o)^2 \times [\partial u_x(x,y)/\partial x]^2 + 1/4fk(\Phi q_x{}^0)^2 \times [u_x(x,y) - \upsilon_x(x,y)]^2\}. \quad (7)$$

The first term is the out-of-plane bending energy. The second and third terms are, respectively, in-plane bending and compression energies of the straight 1D wave fronts of a fluctuating undulated lipid bilayer. The last term results from the displacement of the straight 1D wave fronts of the undulated lipid bilayer relative to the displacements of the ordered in-phase F-actin monolayer perpendicular to the straight 1D wave fronts. These emerging free energy terms are modulated by the amplitude of induced undulation of the fluid lipid bilayer, their energy scales being proportional to f^2 or f. A phenomenological Hamiltonian similar to (7) was proposed [23] to study the anomalous elasticity of unidirectionally tethered and rippled membranes, with the exception of the last term in (7).

The elastic fluctuation Hamiltonian H_t for the multilamellar stacking of undulated lipid bilayers and in-phase ordered F-actin monolayers is $H_0 + H_i$ with

$$H_0 = 1/2\sum_n a \iint dxdy\{K_l[\nabla^2 h^n]^2 + 4\xi^4 f^2(\mathrm{K}_{uv}/a^2) \times [\partial^2 u_x{}^n(x,y)/\partial y^2]^2 + B_l{}^e[\partial u_x{}^n(x,y)/\partial x]^2 + \mathrm{K}_{ac}[\partial^2 v_z{}^n/\partial x^2]^2 + B_{ac}[\partial v_x{}^n/\partial x]^2\}, \quad (8)$$

$$H_i = \sum_n a \iint dxdy\{(B_{3d}/a^2)[(h^{n+1} - v_z{}^n)^2 + (v_z{}^n - h^n)^2] + f\mathrm{K}_{uv}/a^2[(u_x{}^{n+1} - v_x{}^n)^2 + (v_x{}^n - u_x{}^n)^2]. \quad (9)$$

Many of the physical parameters entering (8) and (9) may be estimated from measured elastic parameters of the lipid bilayer and F-actin microfilament. $K_l[\approx 0.2(k_BT)/\mathrm{nm}]$ is K_b/a. K_{ac} is $\mathrm{K}_{ac}{}^0/ac$, $\mathrm{K}_{ac}{}^0$ is the bending modulus of a single F-actin. The measured modulus $\mathrm{K}_{ac}{}^0$ shows a wide range of values from $17 \pm 13 \times 10^3 (k_BT)$ nm [24–28]. A recent computational multilevel study of the parameters for F-actin has considerably narrowed down this spread [29,30] pointing to an estimate of $14.4 \times 10^3 (k_BT)$ nm ($\mathrm{K}_{ac} \approx 72\ (k_BT)/\mathrm{nm}$). $B_{ac}(\approx 48(k_BT)/\mathrm{nm}^3)$ is the compression modulus of the F-actin layer stacking [26,29,31] as defined in (8). The in-plane bending rigidity $f^2\xi^4\mathrm{K}_{uv}/a^2(\approx 1.4\times 10^{-3} k_BT/\mathrm{nm})$ equals $1/4 f^2(\xi^4 k/a)\times (q_x{}^0\Phi)^2$. The in-plane compression modulus $B_l{}^e$ ($\approx 0.72 \times 10^{-2}(k_BT)/\mathrm{nm}^3$) equals $12\ (q_x{}^0)^2\xi^4 f^2(\mathrm{K}_{uv}/a^2)$. B_{3d} is the bulk modulus of the multilamellar stacking.

H_t is converted into an effective Hamiltonian H_t^{eff} for a multilamellar stacking of dressed F-actin monolayers by integrating over the fluctuating variables $h(\mathbf{q})$ and $u_x(\mathbf{q})$ of the lipid bilayers. This Hamiltonian for dressed F-actin monolayers has no shear elastic term in the x-z plane. Consequently, the 2D centered rectangular crystalline phase in the x-z plane will emerge from higher order direct interactions between nearest neighboured fluctuating dressed F-actin monolayers that set them into longitudinal spatial registry as exemplified in Ref. [12] for transversal registry in DNA complexes with the elastic Hamiltonian for a centered rectangular columnar lattice [32].

To capture the essence of the structurally ordered phase, returning to $H_t{}^{\mathrm{eff}}$, we obtain an effective Hamiltonian for the elastic fluctuations $v_x{}^n(x,y)$ by integrating over the fluctuating variables $v_z{}^n(x,y)$. This leads to $\tilde{H}_t{}^{\mathrm{eff}}(\mathbf{q})$ given by

$$\tilde{H}_t{}^{\mathrm{eff}}(\mathbf{q}) = \tilde{A}_{vx}(\mathbf{q}) v_x(\mathbf{q}) v_x(-\mathbf{q}), \quad (10)$$

with $\tilde{A}_{vx}(\mathbf{q})$ which, in the small-$\mathbf{q_2}$ limit, becomes

$$\tilde{A}_{vx}(\mathbf{q}) = 2(f\mathrm{K}_{uv}/a^2)(1 - \cos q_z a) + 2(f^2\mathrm{K}_{uv}/a^2)\xi^4 q_y{}^4(1 + \cos q_z a) + [B_{ac} - 8(\mathrm{K}_{uv}/a^2)\xi^4 (q_x{}^0)^2] q_x{}^2. \quad (11)$$

The coefficient of $q_x{}^2$ is independent of q_z and may be clearly taken equal to B_{ac}. Converting back to real space, $\tilde{H}_t{}^{\mathrm{eff}}$ is

$$\tilde{H}_t{}^{\mathrm{eff}} = 1/2\sum_n a \iint dxdy\{B_{ac}[\partial v_x{}^n/\partial x]^2 + K_y[\partial^2 v_x{}^n/\partial y^2]^2 + B_z[(v_x{}^{n+1} - v_x{}^n)/a]^2\}. \quad (12)$$

B_z equals fK_{uv}. K_y, the intralayer bending term, equals to $4f^2(K_{uv}/a^2)\xi^4$. This effective elastic Hamiltonian for the elastic variable $v_x(x,y,z)$ is typical of three-dimensional highly anisotropic columnar liquid crystal, the lines formed by the straight 1D wave fronts (y direction) playing the role of the columns of molecules. The mean square displacement thermal average $\langle v_x{}^2(x,y,z)\rangle$ stays finite when the size of the sample goes to infinity and is given by [33]:

$$\langle v_x{}^2(x,y,z)\rangle = (k_BT/4\pi\sqrt{2})(\lambda_B/B_{ac})(q_c/\lambda)^{1/2}. \quad (13)$$

$\lambda_B{}^2 = B_{ac}/B_z$, $\lambda^2 = K_y/B_{ac}$ and q_c is the cutoff at $2\pi/b$. Using the values of the parameters reported above, $[\langle v_x{}^2(x,y,z)\rangle]^{1/2}$ is a fraction of a nanometer, less than a tenth of the basic period. The result (13) leads to true two-dimensional Bragg peaks as observed experimentally [3].

For completeness, an effective Hamiltonian for dressed mixed lipid bilayers is obtained by integrating out the elastic variables of the F-actin monolayers in (8) and (9). In addition, by integrating out the variables $h(\mathbf{q})$, the following effective Hamiltonian for the in-plane elastic variables $u_x(\mathbf{q})$ of the dressed mixed lipid bilayers is obtained:

$$H^{\mathrm{eff}}\{u_x\} = 1/2 \iiint d\mathbf{q}/(2\pi)^3 [B_{ac} q_x{}^2 + fK_{uv} q_z{}^2 + 4f^2\xi^4 (K_{uv}/a^2) q_y{}^4] u_x(\mathbf{q}) u_x(-\mathbf{q})]. \quad (14)$$

This is typical of a highly anisotropic columnar liquid crystal with the columnar axis pointing perpendicular to the F-actin axis in the midplane of the lipid bilayers. As expected, long range order sets in the plane formed by the F-actin axis and the axis perpendicular to the midplanes of the undulated lipid bilayers [Fig. 1(a)]. By integrating over the variables $u_x(\mathbf{q})$ instead of $h(\mathbf{q})$, we get an effective Hamiltonian for the out-plane elastic variables $h(\mathbf{q})$ which is

$$H^{\mathrm{eff}}\{h\} = 1/2 \iiint d\mathbf{q}/(2\pi)^3 [(K_{ac} + K_l) q_x{}^4 + 2K_l q_x{}^2 q_y{}^2 + K_l q_y{}^4 + B_{3d} q_z{}^2] h(\mathbf{q}) h(-\mathbf{q}). \quad (15)$$

This is the typical form for the out of plane fluctuations for a multilamellar stack of lipid bilayers that have developed a highly anisotropic bending energy term. This anisotropy imposed by the bending rigidity K_{ac} of the F-actin strands will considerably modified the out of plane thermal fluctuations of the dressed bilayers at shorter length scales [6], leading to observable deviations from the classical Caillé line shape of lamellar Bragg peaks [34]. This is an additional physical signature that should be experimentally observed to confirm our model.

A new mechanism is proposed to set F-actins into longitudinal registry in the lamellar phase of mixed fluid lipid bilayers and F-actin monolayers. The in-phase longitudinal order of F-actin monolayers and the longitudinal undulation of the lipid bilayers mutually lock each other leading to an in-plane curvature energy term which is proportional to the squared amplitude of the static lipid bilayer. This term turns the soft-matter complex into a full analogue of a highly anisotropic columnar liquid crystal. The corresponding structure was recently observed in Ref. [3] and also fits well the primary diffraction data reported earlier in Ref. [13]. This conclusion is strongly supported by a quantitative analysis based on independent measured values of physical parameters of F-actin. The above mechanism is set into action for the lipid bilayer and F-actin complex, contrary to the corresponding complex with DNA, because of the highly modulated transverse cross section of F-actin and the larger value of its pitch (36 nm compared to 3.4 nm for DNA). This is first time reported evidence of in-plane longitudinal ordering of elongated and rigid macro-ions and their setting into registry.

The proposed mechanism suggests the possibility for membrane-induced bundling of F-actin and longitudinally ordered microstructures [4] at the plasma membrane. Finally, for mixed lipid bilayers and F-actin, a helical phase of twisted lamellae cannot be ruled out and raises the attractive question of how the chiral symmetry of F-actin can propagate through membrane deformations at macroscopic length scale. Consequently, in this context, a transition [35] for such a chiral biomacromolecule and lipid bilayer complex from helical "fibrillar" twisted phases of finite size to the unbounded achiral crystalline phase reported above has to be envisaged.

A. C. wishes to thank the "Institut Curie" for its kind hospitality which has allowed for this work to be completed. A. C. and F. A. thank Jean-François Joanny for very useful discussions on the subject of this Letter, Roberto Dominguez for sharing information on actin electrostatics and kindly providing us with a high resolution model of the actin microfilament [19], and the late P. G. de Gennes for inspiring discussions on crystalline states and molecular symmetries, at the early stage of this work. This work is supported by a grant of the Canadian granting NSERC attributed to A. C., and ANR grants to F. A.

[1] M. A. Mintzer and E. E. Simanek, Chem. Rev. **109**, 259 (2009).
[2] N. Zhihong, A. Petukhova, and E. Kumacheva, Nat. Nanotechnol. **5**, 15 (2010).
[3] E. Henry, A. Dif, M. Schmutz, L. Legoff, F. Amblard, V. Marchi-Artzner, and F. Artzner, Nano Lett. **11**, 5543 (2011).
[4] A. P. Allen, D. L. Richmond, L. Maibaum, S. Pronk, P. L. Geissler, and D. A. Fletcher, Nat. Phys. **4**, 789 (2008).
[5] J. O. Rädler, I. Koltover, T. Salditt, and C. R. Safinya, Science **275**, 810 (1997).
[6] T. Salditt, I. Koltover, J. O. Rädler, and C. R. Safinya, Phys. Rev. Lett. **79**, 2582 (1997); Phys. Rev. E **58**, 889 (1998).
[7] F. Artzner, R. Zantl, G. Rapp, and J. O. Rädler, Phys. Rev. Lett. **81**, 5015 (1998).
[8] R. Zantl, F. Artzner, G. Rapp, and J. O. Rädler, Europhys. Lett. **45**, 90 (1999).
[9] I. Koltover, T. Salditt, J. O. Rädler, and C. R. Safinya, Science **281**, 78 (1998).
[10] L. Golubovic and M. Golubovic, Phys. Rev. Lett. **80**, 4341 (E) (1998); **81**, 5704 (1998).
[11] C. S. O'Hern and T. C. Lubensky, Phys. Rev. Lett. **80**, 4345 (1998).
[12] L. Golubovic, T. C. Lubensky, and C. S. O'Hern, Phys. Rev. E **62**, 1069 (2000).
[13] G. C. L. Wong, J. X. Tang, A. Lin, Y. Li, P. A. Janmey, and C. R. Safinya, Science **288**, 2035 (2000).
[14] E. H. Egelman, J. Muscle Res. Cell Motil. **6**, 129 (1985).
[15] K. C. Holmes, D. Popp, W. Gebhard, and W. Kabsch, Nature (London) **347**, 44 (1990).
[16] T. Ikawa, F. Hoshino, O. Watanabe, Y. Li, P. Pincus, and C. R. Safinya, Phys. Rev. Lett. **98**, 018101 (2007).
[17] T. Oda, M. Iwasa, T. Aihara, Y. Maéda, and A. Narita, Nature (London) **457**, 441 (2009).
[18] T. Fujii, A. H. Iwane, T. Yanagida, and K. Namba, Nature (London) **467**, 724 (2010).
[19] R. Dominguez and K. C. Holmes, Annu. Rev. Biophys. **40**, 169 (2011).
[20] S. Leibler and D. Andelman, J. Phys. (Paris) **48**, 2013 (1987).
[21] P. S. Swain and D. Andelman, Langmuir **15**, 8902 (1999).
[22] M. Manghi and N. Destainville, Langmuir **26**, 4057 (2010).
[23] J. Toner, Phys. Rev. Lett. **74**, 415 (1995).
[24] S. Fujime and S. Ishiwata, J. Mol. Biol. **62**, 251 (1971).
[25] R. Yasuda, H. Miyata, and K. Kinosita, Jr., J. Mol. Biol. **263**, 227 (1996).
[26] F. Gittes, B. Mickey, J. Nettleton, and J. Howard, J. Cell Biol. **120**, 923 (1993).
[27] O. Panke, D. A. Cherepanov, K. Gumbiowski, K. Engelbrecht, and S. Junge, Biophys. J. **81**, 1220 (2001).
[28] L. LeGoff, O. Hallatschek, E. Frey, and F. Amblard, Phys. Rev. Lett. **89**, 258101 (2002).
[29] M. A. Deriu, T. C. Bidone, F. Mastrangelo, G. Di Benedetto, M. Soncini, F. M. Montevecchi, and U. Morbiducci, J. Biomech. **44**, 630 (2011).
[30] M. A. Deriu, A. Shkurti, G. Paciello, T. C. Bidone, U. Morbiducci, E. Ficarra, A. Audenino, and A. Acquaviva, Proteins **80**, 1598 (2012).
[31] H. Kojima, A. Ishijima, and T. Yanagida, Proc. Natl. Acad. Sci. U.S.A. **91**, 12 962 (1994).
[32] H. Brand and H. Pleiner, Phys. Rev. A **24**, 2777 (1981).
[33] P. G. de Gennes and J. Prost, *The Physics of Liquid Crystals* (Oxford University Press, Oxford, 1993).
[34] A. Caillé, C. R. Acad. Sci., Paris **274**, 891 (1972).
[35] T. P. J. Knowles, A. De Simone, A. W. Fitzpatrick, A. Baldwin, S. Meehan, L. Rajah, M. Vendruscolo, M. E. Welland, C. M. Dobson, and E. M. Terentjev, Phys. Rev. Lett. **109**, 158101 (2012).